RESEARCH ARTICLE

J Anim Sci Technol 2024;66(4):702-716
https://doi.org/10.5187/jast.2023.e104

JAST
Journal of Animal Science and Technology
pISSN 2672-0191 eISSN 2055-0391

Weighted single-step genome-wide association study to reveal new candidate genes for productive traits of Landrace pig in Korea

Jun Park, Chong-Sam Na*

Department of Animal Biotechnology, Jeonbuk National University, Jeonju 54896, Korea

Received: Jul 14, 2023
Revised: Sep 12, 2023
Accepted: Oct 4, 2023

***Corresponding author**
Chong-Sam Na
Department of Animal Biotechnology, Jeonbuk National University, Jeonju 54896, Korea.
Tel: +82-63-270-2607
E-mail: csna@jbnu.ac.kr

Copyright © 2024 Korean Society of Animal Sciences and Technology. This is an Open Access article distributed under the terms of the Creative Commons Attribution Non-Commercial License (http://creativecommons.org/licenses/by-nc/4.0/) which permits unrestricted non-commercial use, distribution, and reproduction in any medium, provided the original work is properly cited.

ORCID
Jun Park
https://orcid.org/0000-0003-2682-5177
Chong-Sam Na
https://orcid.org/0000-0002-8979-5633

Competing interests
No potential conflict of interest relevant to this article was reported.

Funding sources
Not applicable.

Acknowledgements
Not applicable.

Availability of data and material
Upon reasonable request, the datasets of this study can be available from the corresponding author.

Abstract

The objective of this study was to identify genomic regions and candidate genes associated with productive traits using a total of 37,099 productive records and 6,683 single nucleotide polymorphism (SNP) data obtained from five Great-Grand-Parents (GGP) farms in Landrace. The estimated of heritabilities for days to 105 kg (AGE), average daily gain (ADG), backfat thickness (BF), and eye muscle area (EMA) were 0.49, 0.49, 0.56, and 0.23, respectively. We identified a genetic window that explained 2.05%–2.34% for each trait of the total genetic variance. We observed a clear partitioning of the four traits into two groups, and the most significant genomic region for AGE and ADG were located on the *Sus scrofa* chromosome (SSC) 1, while BF and EMA were located on SSC 2. We conducted Gene ontology (GO) and Kyoto Encyclopedia of Genes and Genomes (KEGG), which revealed results in three biological processes, four cellular component, three molecular function, and six KEGG pathway. Significant SNPs can be used as markers for quantitative trait loci (QTL) investigation and genomic selection (GS) for productive traits in Landrace pig.

Keywords: Gene ontology, Kyoto Encyclopedia of Genes and Genomes, Landrace pigs, Productive traits, Weighted single-step genome-wide association studies

INTRODUCTION

Pig breeding for economic traits has undergone continuous improvement over time, with ongoing research in this field. Productive traits such as average daily gain (ADG), days to 105 kg (AGE), and backfat thickness (BF) have moderate to high heritability. ADG and AGE directly influence pig growth [1, 2]. BF is a trait linked to reproductive performance of Landrace and Yorkshire sows [3], making it crucial for enhancing and maintaining mothering ability of the dam.

According to the Korean Swine Performance Recording Standards (KSPRS) established by the Ministry of Agriculture, Food and Rural Affairs (MAFRA), performance testing is conducted within a weight range of 70–110 kg, with the endpoint set at 90 kg. Days to reach 90 kg and BF are adjusted to assess growth trait performance. However, the endpoint weight of 90 kg has remained unchanged since its establishment in 1984, reflecting the market weight of finishing pigs at that time. With current trend of market weights surpassing 110 kg, there is a growing consensus that the endpoint weight for

Authors' contributions
Conceptualization: Park J, Na CS.
Data curation: Park J.
Formal analysis: Park J
Methodology: Park J, Na CS.
Software: Park J.
Validation: Na CS.
Investigation: Na CS.
Writing - original draft: Park J.
Writing - review & editing: Park J, Na CS.

Ethics approval and consent to participate
This article does not require IRB/IACUC approval because there are no human and animal participants.

performance testing should be increased. Consequently, there is a need to develop a new adjustment formula for performance testing, resulting in the creation of a 105 kg-based adjustment formula by the National Institute of Animal Science (NIAS).

Genome-wide association studies (GWAS) have been widely applied in various fields, including the identification of economic traits. Multiple candidate genes and significant markers have been reported for the same trait, with associations between multiple traits observed at the same locus. These results are inherent to quantitative traits, single-marker GWAS analyses might have limited power for detecting quantitative trait loci (QTLs) and mapping accuracy [4]. The cost of analyzing single nucleotide polymorphism (SNP) panels and the imbalance between individuals with genomic data and those without genomic data present additional limitations.

The weighted single-step (Wss)GWAS method has emerged as a powerful approach that leverages genomic estimated breeding values (GEBVs) derived from genotypes, phenotypes, and pedigree information to estimate the effects of SNPs [5]. This method effectively addresses the issue of unequal variances among SNPs, leading to more accurate estimation of SNP effects [6]. WssGWAS is more effective than GWAS in analyzing traits that are influenced by QTLs with significant effects or when there is insufficient phenotype and genotype data available. Recent studies have successfully used this approach to identified various economic traits in livestock species [7–9].

We investigate the genetic regions and candidate genes associated with productive traits (adjusted to 105 kg body weight) in Landrace pig using WssGWAS. Also, we conducted GO and KEGG enrichment analyses to gain deeper insights into the underlying biological processes and functional terms associated with the identified candidate genes for productive traits.

MATERIALS AND METHODS

Ethical approval

This article does not require IRB/IACUC approval because there are no human and animal participants.

Animals and phenotypes

We obtained the total 37,099 productive records (9,818 males and 27,281 females) born from 2015 to 2021 at five Great-Grand-Parents (GGP) farms (Supplementary Table S1). We adjusted to evaluate for productive traits (AGE, ADG, BF, and eye muscle area [EMA] to 105 kg) with method outlined by the NIAS in Korea (https://www.nias.go.kr/images/promote/result/file/2021_2_5.pdf), and the equations used are as follows:

$$\text{Adjusted AGE} = \text{Measure age} - \frac{(105 - \text{measure weight}) \times (\text{measure age} - \alpha)}{\text{Measure weight}}$$

where α is the correction factor used to adjust AGE to 105 kg as follows:

$$\alpha : \textit{Sire} = 63.3; \textit{Dam} = 47.3$$

ADG adjusted to 105 kg is calculated using the following equation:

$$\text{Adjusted ADG} = \frac{105\text{kg}}{\text{Adjusted AGE}}$$

BF adjusted to 105 kg is calculated using the following equation:

$$\text{adjusted BF} = \text{Measure BF} \times \frac{(105 - \text{measure weight}) \times (\text{measure BF} - \beta)}{\text{measure weight}}$$

where β is the correction factor used to adjust BF to 105kg as follows:

$$\beta : Sire = 2.6;\ Dam = 3.7$$

EMA adjusted to 105 kg is calculated using the following equation:

$$\text{adjusted EMA} = \text{Measure EMA} \times \frac{(105 - \text{measure weight}) \times (\text{measure EMA} - \gamma)}{\text{measure weight}}$$

where γ is the correction factor used to adjust EMA to 105kg as follows:

$$\gamma : Sire = 29.1;\ Dam = 33.0$$

Single nucleotide polymorphism data and quality control

Illumina Porcine 60K V1 and V2 were used and V2 was selected as a reference panel for imputation. Prior to imputation, phasing was performed using Shapeit4 [10], a fast and accurate method for haplotype estimation using a positional Burrows-Wheeler transform (PBWT)-based approach to select informative conditioning haplotypes. Imputation was then conducted using Impute5 [11], assuming phased samples having no missing alleles. After imputation, quality control (QC) was performed by PLINK v1.09 [12] to exclude SNPs with low call rates (< 90%), low minor allele frequencies (< 0.01), or deviation from Hardy-Weinberg equilibrium (10^{-6}). After QC, we used the number of animals and SNPs were 6,683 and 35,420, respectively.

Statistical analysis

We estimated the genetic parameters for AGE, ADG, BF, and EMA with average information restricted maximum likelihood (AIREML) method. We considered two approaches: pedigree-based best linear unbiased prediction (PBLUP) and single-step genomic best linear unbiased prediction (ssGBLUP). Each trait was estimated with a single-trait animal model, and the equation as follows:

$$y = Xb + Za + e$$

where y is the vector of observations; b is the vector of fixed effects (herd-birth year-season, sex); a is the vector of additive genetic effects; e is the vector of residuals; and X and Z are the incidence matrices for b, a, and e. Heritability was estimated as $h^2 = \frac{\sigma_a^2}{\sigma_a^2 + \sigma_e^2}$, where σ_a^2 and σ_e^2 were additive genetic and residual variances, respectively.

Furthermore, GEBVs calculated using ssGBLUP approach, and marker effects were derived from these GEBVs. In contrast to the conventional BLUP approach, ssGBLUP substituted the inverse of the pedigree relationship matrix (A^{-1}) with the inverse of the combined matrix H^{-1}, which incorporated both the pedigree and genomic relationship matrices [13]. The H^{-1} can be represented as follows:

https://doi.org/10.5187/jast.2023.e104

$$H^{-1} = A^{-1} + \begin{bmatrix} 0 & 0 \\ 0 & G^{-1} - A_{22}^{-1} \end{bmatrix}$$

where A_{22}^{-1} is the inverse of numerator relationship matrix for pigs with genotyped, and G refers to the genomic relationship matrix [14]. G is presented below:

$$G = \frac{ZDZ'}{\sum_{i=1}^{M} 2p_i(1-p_i)}$$

where Z is a matrix of gene content adjusted for allele frequencies (0, 1 or 2 for *AA*, *Aa* and *aa*, respectively), *D* is a diagonal matrix of weights for SNP variances (initially *D* = *I*), *M* is the number of SNPs, and p_i is the minor allele frequency of i^{th} SNP. Estimates of SNP effects and weights for WssGWAS were obtained according to following steps [5]:

1. First step (t = 1): $D = I$, $G_{(t)} = D_{(t)}Z'\lambda$, where $\lambda = \frac{1}{\sum_{i=1}^{M} 2p_i(1-p_i)}$ [5];
2. Calculate GEBVs;
3. Convert GEBVs to SNP effects $(\hat{u}): u = \lambda D_{(t)}Z'G_{(t)}^{-1}a_g$, where a_g was the GEBV of animal that was also genotyped;
4. Calculate the weight for each SNP: $d_{i(t+1)} = \hat{u}_{i(t)}^2 2p_i(1-p_i)$, where i was the i^{th} SNP;
5. Normalize SNP weights to keep the total genetic variance constant:

$$D_{(t+1)} = \frac{\mathrm{tr}(D_{(1)})}{\mathrm{tr}(D_{(t+1)})} D_{(t+1)}$$

6. $G_{(t+1)} = ZD_{(t+1)}Z'\lambda$ was calculated;
7. $t = t + 1$ and loop to step 2.

The procedure was iteratively performed for a total of three cycles, taking into account the achieved accuracies of GEBV [15,16]. During each iteration, the weights of SNPs were updated (steps 4 and 5), and utilized to construct G matrices (step 6), update GEBV (step 2), and estimate SNP effects (step 3). Subsequently, the proportion of genetic variance explained by each consecutive set of SNPs, referred to as i^{th} SNP windows, was calculated [16]. In a previous study, values for α_i were determined based on linkage disequilibrium (LD) decay distance analysis of the population, considering the distance where r^2 drops below 0.2 [17]. In this study, LD decay distance was not calculated separately, and to facilitate comparison with the previous study's findings [17], the same value of 0.8 Mb was adopted. SNPs were positioned within a 0.8 Mb region, and the percentage of genetic variance explained by each 0.8 Mb window was determined as follows:

$$\frac{\mathrm{Var}(a_i)}{\sigma_a^2} \times 100 = \frac{\mathrm{Var}\left(\sum_{j=1}^{x} Z_j \hat{u}_j\right)}{\sigma_a^2}$$

where α_i is the genetic value of the i^{th} SNP window that consisted of a region of consecutive SNPs located within 0.8 Mb, σ_a^2 was the total additive genetic variance, Z_j was the vector of gene

content of the j^{th} SNP for all individuals, and $\hat{u}_j$ was the effect of the j^{th} SNP within the i^{th} window. To visualize the distribution of these SNP windows, Manhattan plots were generated using the R software and CMplot package [18,19]. The procedures described above were implemented iteratively using the software suite of BLUPF90 programs [20].

Identification of candidate genes and functional enrichment analysis

We conducted to identify specific genomic regions associated with productive traits by examining QTL using genomic windows that accounted for more than 1.0% of the total genetic variance.

These genomic windows, previously employed in similar studies [17], represent regions of the genome that contribute significantly to the genetic variation underlying productive traits.

Our focus on these candidate QTL regions aimed to uncover genetic markers or regions that play a pivotal role in influencing growth-related characteristics. Notably, we observed a significant deviation from the expected average genetic variance explained by the 0.8 Mb window, which accounted for 0.0495% of the genetic variance on average (dividing 100% by the number of 2022 genomic regions). The 1% threshold exceeded the anticipated average genetic variance explained by the 0.8 Mb window by more than 20-times. To identify genes within the identified QTL regions, particularly within the significant windows, we utilized the ensemble *Sus scrofa* 11.1 database (https://www.ensembl.org/biomart). Furthermore, to gain deeper insights into the biological processes associated with these regions, we performed gene ontology (GO) and Kyoto Encyclopedia of Genes and Genomes (KEGG) analyses using the Database for Annotation, Visualization, and Integrated Discovery (DAVID v6.8, https://david.ncifcrf.gov/). GO terms and KEGG pathways showing significant enrichment were determined based on a p-value threshold of < 0.05. Through these analyses, we gained valuable knowledge regarding crucial molecular pathways and biological functions associated with the observed genetic variations.

RESULTS AND DISCUSSION

Variance component and heritability

The estimates of the heritabilities for AGE, ADG, BF, and EMA were 0.49, 0.49, 0.56, and 0.23, respectively (Table 1). Results showed that the heritability of ssGBLUP was higher than that of PBLUP, which only used pedigree information. The ssGBLUP method, which incorporates both pedigree and genetic information, theoretically provides more accurate estimates of genetic parameters [7].

Table 1. Variance components and heritabilities for productive traits

Traits	Method	σ_a^2	σ_e^2	σ_P^2	h^2 (SE)
AGE (days)	PBLUP	47.66	58.18	105.84	0.45 (0.01)
	ssGBLUP	54.130	56.73	110.86	0.49 (0.01)
ADG (g)	PBLUP	766.41	923.76	1,690.20	0.45 (0.01)
	ssGBLUP	889.23	890.09	1,779.30	0.49 (0.01)
BF (mm)	PBLUP	3.69	3.40	7.109	0.52 (0.01)
	ssGBLUP	4.18	3.27	7.46	0.56 (0.01)
EMA (cm^2)	PLBUP	1.89	6.46	8.34	0.22 (0.01)
	ssGBLUP	1.96	6.50	8.45	0.23 (0.01)

σ_a^2, additive genetic. σ_e^2, residual. σ_P^2, phenotypic variances. h^2 (SE), heritability and standard error; AGE, days to 105 kg; PBLUP, pedigree-based best linear unbiased prediction ; ssGBLUP, single-step genomic BULP; ADG, average daily gain; BF, backfat thickness; EMA, eye muscle area.

https://doi.org/10.5187/jast.2023.e104

Genome-wide association study

In most cases, major economic traits of livestock are quantitative traits except for some traits. These quantitative traits are characterized by a complex genetic structure. Exploration of candidate genes for such traits has always been an important goal of animal breeding programs. In this study, the genetic variance explained by a 0.8 Mb window for each growth trait was estimated using WssGWAS (Fig. 1). Specifically, we explained 2.05%, 3.23%, 9.27%, and 9.96% of the total genetic variation for AGE, ADG, BF, and EMA, respectively, with the most significant window explaining approximately 2.05%–2.34% of the total genetic variation (Table 2). Furthermore, within the identified window regions of this study, we presented the SNP markers, their corresponding chromosome (Chr), positions, and the associated genetic variance values explained by each marker (Supplementary Tables S2, S3, S4 and S5).

Previous GWAS studies have reported significance regions on *Sus scrofa* chromosome (SSC) 1, 3, 6, 8, and 13 for ADG and on SSC 1, 3, 6, 8, and 10 for AGE, explaining a total of 8.09% and 4.08% of the genetic variance, respectively [21]. Moreover, candidate QTL regions on SSC 4 and 14 for AGE, on SSC 4 and 2 for ADG, and on SSC 2, 3, and 10 for BF explain a total of 6.48%, 5.96%, and 6.76% of genetic variance, respectively [4]. The utilization of the WssGWAS, which incorporates SNP windows for genetic variance estimation, offers improved capabilities in

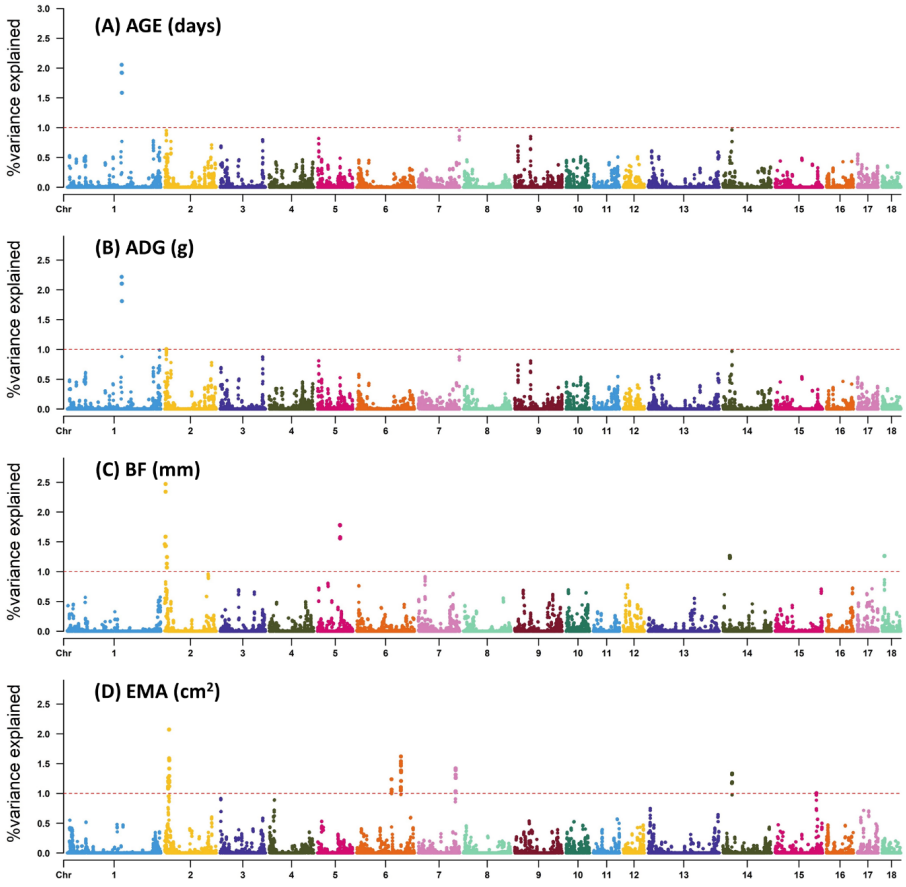

Fig. 1. Proportion of genetic variances of productive traits explained by 0.8 Mb windows. AGE, days to 105 kg; ADG, average daily gain; BF, backfat thickness; EMA, eye muscle area.

Table 2. Significance regions and candidate genes for productive traits

Traits	SSC	Position (Mb)	gVar (%)[1)]	nSNP	Candidate genes
AGE (days)	1	159.24–159.88	2.05	9	*RELCH, PIGN, RNF152, CDH20*
ADG (g)	1	159.24–159.88	2.22	9	*RELCH, PIGN, RNF152, CDH20*
	2	4.97–5.71	1.01	10	*NDUFV1, CABP4, CORO1B, PTPRCAP*
BF (mm)	2	2.46–3.26	2.34	15	*ACTE1, SHANK2, CTTN, ANO1*
		0.07–0.42	1.46	5	*PSMD13, COX8H*
		6.64–7.42	1.25	24	*MAP3K11*
	5	65.61–66.36	1.68	18	*NDUFA9, AKAP3, DYRK4, RAD51AP1,FGF6, C12orf4, TIGAR*
	14	19.67–20.42	1.27	10	*AADAT, MFAP3L, CLCN3, NEK1, SH3RF1*
	18	6.88–7.67	1.27	28	*ZYX, FAM131B*
EMA (cm^2)	2	13.04–13.46	2.07	21	*CTNND1, BTBD18, TMX2, MED19, SERPING1*
		10.19–10.99	1.26	23	*DDB1, VWCE, PPAG3*
	6	129.64–130.41	1.62	21	*TTLL7, ADGRL2*
		102.18–102.96	1.24	13	*AKAIN1, DLGAP1*
	7	109.35–110.14	1.42	24	*ENSSSCG00000052115, ENSSSCG00000037928*
	14	26.65–27.30	1.34	13	*TMEM132C, ENSSSCG00000042937*
	15	121.01–121.81	1.01	15	*CRYBA2, CFAP65, IHH*

[1)]Represents the proportion of genetic variance explained by 0.8 Mb.

SSC, Sus scrofa chromosome; nSNP, number of SNP in region; AGE, days to 105 kg; ADG, average daily gain; BF, backfat thickness; EMA, eye muscle area.

identifying previously unknown QTLs compared to conventional GWAS methods. This approach mitigates the risk of overestimating the number of detected QTLs and false positives resulting from LD [22,23]. Furthermore, the iterative weighting of SNPs enhances the detection of QTLs with larger effects [16]. In this study, a total of 10 iterations were conducted, and the genomic accuracy for each trait was presented (Supplementary Table S6). As the number of iterations increased, there was a corresponding increase in genetic accuracy, consistent with previous study [5]. The highest increase was observed at the 3rd iteration, followed by a gradual decrease. Unlike the study that reported a decrease in weights at certain iterations [5], our study showed an increase in accuracy up to 0.02 to 0.04 over 10 iterations, as compared to the first iteration where all SNP weights were set to I. While the optimal number of iterations for each trait was not conclusively determined in our study, we chose to use the results from the 3rd iteration, which exhibited the highest genetic accuracy, for the GWAS analysis.

Candidate gene for days to 105 kg and average daily gain

We have successfully identified three significant regions (SSC 1, 7, and 14) that are associated with AGE. These regions explain 1.03%–2.03% of the total genetic variance for AGE. Additionally, we conducted gene annotation and identified five genes with potential as candidate genes. Similarly, ADG is discovered five relevant QTL regions (SSC 1, 2, 7, and 14) that account for 1.01%–2.14% of the total genetic variance. Within these regions, we have annotated seven genes. Notably, although three QTL regions associated with AGE are also found to be associated with ADG, the proportions of genetic variance explained differ between the two traits.

When considering complex quantitative traits, it is important to acknowledge that linear gene effects may not consistently align with average trait values. Instead, a nonlinear assumption is often more appropriate [21], as gene contributions can exhibit nonlinearity and pleiotropic effects between traits may manifest [4]. Pleiotropic QTLs are prevalent in the porcine genome,

https://doi.org/10.5187/jast.2023.e104

as exemplified by the presence of QTLs associated with vertebral number, body length, and nipple number on SSC 7 [24]. Considering the overlap in the identified genomic regions and the substantial genetic correlation observed between ADG and AGE, it is reasonable to infer that the genes associated with these traits are shared.

Within the identified genomic regions, we observed the presence of *RELCH* in close proximity to *MC4R* on SSC 1. *RELCH* has been previously recognized as one of the seven potential candidate genes associated with pig fatness traits [25] and has demonstrated an association with pig fat depth [26]. Functionally, *RELCH* is involved in regulating intracellular cholesterol distribution, specifically from recycling endosomes to the trans-Golgi network. GO analysis further revealed enrichment in biological processes related to neuroactive ligand-receptor interaction [27]. These findings provide valuable insights into the potential regulatory mechanisms underlying fatness traits in pigs and highlight the role of *RELCH* in cholesterol metabolism and neuroactive signaling pathways.

RNF152 emerges as a promising candidate gene associated with pig fatness and body composition traits [25,26], specifically BF in Duroc pigs as revealed by ssGWAS analysis [28]. This gene acts as a negative regulator of the mammalian target of rapamycin (mTOR) signaling pathway [29,30], a key pathway governing cellular metabolism, survival, and proliferation through the regulation of anabolic processes such as protein, lipid, and nucleotide synthesis. The pivotal role of the mTOR pathway in cellular function has been extensively documented [31–34]. Our study highlights the potential pleiotropic effects within the SSC 1 region, which exhibited remarkable significance for both AGE and ADG traits. These findings provide valuable insights into the genetic architecture underlying productive traits and the interplay of key molecular pathways in pigs.

CDH20 has been identified as a candidate gene for pig fatness traits and days to reach 100 kg in previous studies [25, 35]. *CDH20* encodes a type 2 classical cadherin, which is a calcium-dependent cell-cell adhesion glycoprotein and a potential candidate for tumor suppression [36]. Additionally, *CDH20* is involved in the cell adhesion pathway. This study is the first to report its association with porcine growth and fatness traits [37].

TMEM132C has been identified as a potential candidate gene for growth and fatness-related traits in Bamaxiang pigs using a customized 1.4 million SNP array [38]. It has also been implicated as one of the candidate genes for average backfat at 100 kg [39].

NDUFV1 is located in the SSC 2 region and plays a critical role in energy metabolism [40]. Previous investigations have consistently demonstrated a significant downregulation of *NDUFV1* expression in placental tissues, particularly when compared to the control group representing normal pregnancies. Notably, *NDUFV1* plays a crucial role in facilitating energy production within the mitochondrial matrix and membrane, thereby influencing essential metabolic processes [41].

Candidate gene for backfat thickness and eye muscle area

BF had the highest explained genetic variance and identified the highest number of candidate genes. Specifically, six relevant regions located on SSC 2, 5, 14, and 18 were identified, explaining 1.27%–2.34% of the total genetic variance, and 21 genes were annotated. EMA had lower heritability other traits such as AGE, ADG, and BF, but it was moderate heritability. Moreover, the significant genetic regions identified for EMA did not coincide with those found for BF, although SSC 2 and 14 exhibited similar levels of variance explained. Similar to BF, the region with the highest significant genetic variance explained was SSC 2 with 2.07% for EMA, while SSC 6, SSC 7, SC14, and SSC 15 were also identified as regions associated with EMA.

ANO1, also known as *TMEM16A*, is a $Ca2^{+}$-activated chloride channel that plays a vital role in

various physiological functions [42]. This channel is critical for maintaining the *STT* of urinary tract muscles in female mice and women. Sex differences in this context are likely influenced by *ANO1* expression in SMCs of the urethra, and this gene is also involved in smooth muscle contraction [43,44].

PSMD13, also referred to as *S11, Rpn9, p40.5, or HSPC027*, is a 376 amino acid protein belonging to the proteasome subunit S11 family. It is located in the SSC 2 region and has been identified as being associated with loin depth in previous studies [45]. *COX8H* is a candidate gene situated in the SSC 2 region. It has been reported to explain 3.51% and 5.87% of the total genetic variation for BF and lean percent, respectively, in Yorkshire pigs [46]. Additionally, it has been identified as one of the highly expressed genes in intramuscular adipose tissues of Erhualian pigs [47]. *MAP3K11* belongs to the serine/threonine kinase family and plays a crucial role in the FGFR signaling pathway, which regulates cartilage and bone formation [48]. Furthermore, a previous study has suggested a potential association between *MAP3K11* and body weight in sheep [49].

AKAP3, located in the SSC5 region, is a member of the AKAP family. It interacts with the regulatory subunit of PKA [50]. While it has been predominantly studied in sperm and cancer, previous research has shown the expression of *AKAP3* in the longissimus dorsi muscle of pigs [51]. The expression of *AKAP3* in skeletal muscle and its binding to PKA's regulatory subunit have the potential to affect glycogen content in the muscle, thereby impacting meat quality after post-mortem modifications [51]. *FGF6* is a key regulator of skeletal muscle development that influences muscle fiber diameter and intramuscular fat content [52,53]. Additionally, *FGF6* has been employed in gene delivery systems for skeletal muscle repair [54].

ZYX is located in the SSC18 region and is closely associated with multiple QTLs related to tissue and texture characteristics [55]. *ZYX* is a protein present in focal adhesions depending on active fibers and interacts with the actin-crosslinking protein alpha-actinin. *ZYX* is involved in cellular organization, signal transduction, cellular response to mechanical stress, and cell adhesion [56–59]. Structurally, *ZYX* consists of an N-terminal domain that interacts with proteins involved in signal transduction and a C-terminal LIM domain that plays a crucial role in regulating cell proliferation, differentiation, and protein-protein and/or protein-DNA interactions [60].

MED9, located in the SSC 2 region, is an essential gene for the maintenance of white adipose tissues and adipogenesis in *Piscirickettsia salmonis* [61]. *MED9* also interacts with PPARs, which are important for inflammatory processes [62]. Polymorphism in the *SERPING1* gene has been found to be significantly associated with tenderness and pH24 in both dominant and co-dominant models. Furthermore, this gene can influence the postmortem pH of muscle by regulating glycolysis [63].

Gene ontology terms and Kyoto Encyclopedia of Genes and Genomes pathway enrichment analysis

Enrichment analyses uncovered significant associations between multiple terms and productive traits. Specifically, we observed enrichment in three biological processes, four cellular components, three molecular functions, and six KEGG pathways (Table 3). Notably, the most significant GO term was GO:0004190, which pertains to chromatin. Furthermore, the GO:0005509 category, encompassing calcium ion binding, exhibited enrichment for nine candidate genes, constituting the majority of the candidates.

The process of actin filament bundle assembly (GO:0051017) involves the construction of actin filament bundles with varying degrees of tightness and orientation. It represents a vital aspect of cellular structure and function. Notably, the selective sweep gene *AIF1L* emerged as a significant molecule, playing an essential role in cell survival and contributing to proinflammatory activities of

https://doi.org/10.5187/jast.2023.e104

Table 3. Significant gene ontology (GO) terms and Kyoto Encyclopedia of Genes and Genomes (KEGG) pathways associated with productive traits of Landrace pigs ($p < 0.05$)

Gene ontology and KEGG pathway	nGenes	*p*-value	Gene
GO:0051017-actin filament bundle assembly	2	0.02	*CORO1B, RHOD*
GO:1902476-chloride transmembrane transport	3	0.03	*ANO1, ANO9, CLCN1*
GO:0006303-double-strand break repair via nonhomologous end joining	3	0.01	*KDM2A, NHEJ1, PRPF19*
GO:0005886-plasma membrane	7	0.02	*CDH20, CORO1B, PIGN, PTPRCAP, RHOD, SPTBN2, SYT12*
GO:0035861-site of double-strand break	3	0.03	*DDB1, NHEJ1, PRPF19*
GO:0000785-chromatin	5	0.04	*RAD51AP1, CDCA5, CCND2, DPF2, MEN1*
GO:0008076-voltage-gated potassium channel complex	3	0.04	*CTTN, KCNA1, KCNA6*
GO:0004190-aspartic-type endopeptidase activity	6	0.00	*PGA5, pregnancy-associated glycoprotein 2-like, PPAG3, PIP*
GO:0005247-voltage-gated chloride channel activity	2	0.04	*CLCN1, CLCN3*
GO:0005509-calcium ion binding	9	0.04	*EHD1, IHH, NAALADL1, CDH20, CABP4, CAPN1, LTBP3, SYT12, VWCE*
ssc05012: Parkinson disease	6	0.03	*COX8H, NDUFV1, NDUFA9, PSMD13, PRKACB, UBE2L6*
ssc00982: Drug metabolism - cytochrome P450	3	0.04	*GSTK1*
ssc04340: Hedgehog signaling pathway	3	0.04	*IHH, CCND2, PRKACB*
ssc00480: Glutathione metabolism	2	0.04	*glutathione S-transferase P-like*
ssc00980: Metabolism of xenobiotics by cytochrome P450	2	0.04	*glutathione S-transferase P-like*
ssc05204: Chemical carcinogenesis - DNA adducts	2	0.04	*glutathione S-transferase P-like*

immune cells, including monocytes/macrophages and activated T lymphocytes [64,65].

Chloride transmembrane transport (GO:1902476) refers to the movement of chloride across a membrane. Previous studies have implicated *ANO9* as a gene associated with marbling depth in both purebred and crossbred pigs. The genetic region containing this gene accounts for 3.34% of the total genetic variance for loin depth [45]. Additionally, the *CLCN1* gene participates in the transmission of nerve impulses, a crucial cellular communication process involved in the interaction between adipocytes and myogenic cells [66]. The interplay between these cell types is significant for various aspects of growth and development, including the regulation of myogenesis rate and extent, muscle growth, adipogenesis, lipogenesis/lipolysis, and energy substrate utilization [67].

Calcium ion binding (GO:0005509) denotes the process of binding to a calcium ion (Ca^{2+}). Prior research has identified EHD1 as a candidate gene that likely possesses functional relevance to meat quality in Beijing black pigs [68]. Additionally, a GWAS study revealed a significant association between *EHD1* and the meat-to-fat ratio (MFR) [69]. Furthermore, using *EHD1* knockout mice, researchers demonstrated the regulatory role of *EHD1* in cholesterol homeostasis and lipid droplet storage [70].

In conclusion, this study offers novel insights into the genetic basis of productive traits in pigs. The identified biological processes, pathways, and candidate genes serve as valuable resources for future investigations for genetic improvement with these traits. Significant SNPs can be used as markers for QTL investigation and genomic selection (GS) for productive traits in Landrace pig.

SUPPLEMENTARY MATERIALS

Supplementary materials are only available online from: https://doi.org/10.5187/jast.2023.e104

REFERENCES

1. Fontanesi L, Schiavo G, Galimberti G, Calò DG, Russo V. A genomewide association study for average daily gain in Italian Large White pigs. J Anim Sci. 2014;92:1385-94. https://doi.org/10.2527/jas.2013-7059
2. Ding R, Yang M, Wang X, Quan J, Zhuang Z, Zhou S, et al. Genetic architecture of feeding behavior and feed efficiency in a Duroc pig population. Front Genet. 2018;9:220. https://doi.org/10.3389/fgene.2018.00220
3. Vargovic L, Bunter KL, Hermesch S. Economic benefit of additional recording for welfare traits in maternal breeding objectives for pigs. Proc Assoc Advmt Anim Breed Genet. 2021;24:406-9.
4. Ruan D, Zhuang Z, Ding R, Qiu Y, Zhou S, Wu J, et al. Weighted single-step GWAS identified candidate genes associated with growth traits in a Duroc pig population. Genes. 2021;12:117. https://doi.org/10.3390/genes12010117
5. Wang H, Misztal I, Aguilar I, Legarra A, Muir WM. Genome-wide association mapping including phenotypes from relatives without genotypes. Genet Res. 2012;94:73-83. https://doi.org/10.1017/S0016672312000274
6. Zhang X, Lourenco D, Aguilar I, Legarra A, Misztal I. Weighting strategies for single-step genomic BLUP: an iterative approach for accurate calculation of GEBV and GWAS. Front Genet. 2016;7:151. https://doi.org/10.3389/fgene.2016.00151
7. Marques DBD, Bastiaansen JWM, Broekhuijse MLWJ, Lopes MS, Knol EF, Harlizius B, et al. Weighted single-step GWAS and gene network analysis reveal new candidate genes for semen traits in pigs. Genet Sel Evol. 2018;50:40. https://doi.org/10.1186/s12711-018-0412-z
8. Luo H, Hu L, Brito LF, Dou J, Sammad A, Chang Y, et al. Weighted single-step GWAS and RNA sequencing reveals key candidate genes associated with physiological indicators of heat stress in Holstein cattle. J Anim Sci Biotechnol. 2022;13:108. https://doi.org/10.1186/s40104-022-00748-6
9. Brunes LC, Baldi F, Lopes FB, Lôbo RB, Espigolan R, Costa MFO, et al. Weighted single-step genome-wide association study and pathway analyses for feed efficiency traits in Nellore cattle. J Anim Breed Genet. 2021;138:23-44. https://doi.org/10.1111/jbg.12496
10. Delaneau O, Zagury JF, Robinson MR, Marchini JL, Dermitzakis ET. Accurate, scalable and integrative haplotype estimation. Nat Commun. 2019;10:5436. https://doi.org/10.1038/s41467-019-13225-y
11. Rubinacci S, Delaneau O, Marchini J. Genotype imputation using the positional burrows wheeler transform. PLOS Genet. 2020;16:e1009049. https://doi.org/10.1371/journal.pgen.1009049
12. Purcell S, Neale B, Todd-Brown K, Thomas L, Ferreira MAR, Bender D, et al. PLINK: a tool set for whole-genome association and population-based linkage analyses. Am J Hum Genet. 2007;81:559-75. https://doi.org/10.1086/519795
13. Aguilar I, Misztal I, Legarra A, Tsuruta S. Efficient computation of the genomic relationship matrix and other matrices used in single-step evaluation. J Anim Breed Genet. 2011;128:422-8. https://doi.org/10.1111/j.1439-0388.2010.00912.x
14. VanRaden PM. Efficient methods to compute genomic predictions. J Dairy Sci. 2008;91:4414-23. https://doi.org/10.3168/jds.2007-0980
15. Legarra A, Robert-Granié C, Manfredi E, Elsen JM. Performance of genomic selection in mice. Genetics. 2008;180:611-8. https://doi.org/10.1534/genetics.108.088575
16. Wang H, Misztal I, Aguilar I, Legarra A, Fernando RL, Vitezica Z, et al. Genome-wide

https://doi.org/10.5187/jast.2023.e104

association mapping including phenotypes from relatives without genotypes in a single-step (ssGWAS) for 6-week body weight in broiler chickens. Front Genet. 2014;5:134. https://doi.org/10.3389/fgene.2014.00134
17. Zhuang Z, Ding R, Peng L, Wu J, Ye Y, Zhou S, et al. Genome-wide association analyses identify known and novel loci for teat number in Duroc pigs using single-locus and multi-locus models. BMC Genomics. 2020;21:344. https://doi.org/10.1186/s12864-020-6742-6
18. R Core Team R. R: a language and environment for statistical computing. Vienna: R Foundation for Statistical Computing; 2013.
19. Yin L. CMplot: circle manhattan plot. R package version 3.2. GitHub: San Francisco, CA; 2020.
20. Misztal I, Tsuruta S, Strabel T, Auvray B, Druet T, Lee DH. BLUPF90 and related programs (BGF90). In: Proceedings of the 7th World Congress on Genetics Applied to Livestock Production; 2002; Montpellier, France. Communication No. 28-07.
21. Tang Z, Xu J, Yin L, Yin D, Zhu M, Yu M, et al. Genome-wide association study reveals candidate genes for growth relevant traits in pigs. Front Genet. 2019;10:302. https://doi.org/10.3389/fgene.2019.00302
22. Peters SO, Kizilkaya K, Garrick DJ, Fernando RL, Reecy JM, Weaber RL, et al. Bayesian genome-wide association analysis of growth and yearling ultrasound measures of carcass traits in Brangus heifers. J Anim Sci. 2012;90:3398-409. https://doi.org/10.2527/jas.2011-4507
23. Habier D, Fernando RL, Kizilkaya K, Garrick DJ. Extension of the bayesian alphabet for genomic selection. BMC Bioinformatics. 2011;12:186. https://doi.org/10.1186/1471-2105-12-186
24. Li Y, Pu L, Shi L, Gao H, Zhang P, Wang L, et al. Revealing new candidate genes for teat number relevant traits in Duroc pigs using genome-wide association studies. Animals. 2021;11:806. https://doi.org/10.3390/ani11030806
25. Zeng H, Zhong Z, Xu Z, Teng J, Wei C, Chen Z, et al. Meta-analysis of genome-wide association studies uncovers shared candidate genes across breeds for pig fatness trait. BMC Genomics. 2022;23:786. https://doi.org/10.1186/s12864-022-09036-z
26. Heidaritabar M, Bink MCAM, Dervishi E, Charagu P, Huisman A, Plastow GS. Genome-wide association studies for additive and dominance effects for body composition traits in commercial crossbred Piétrain pigs. J Anim Breed Genet. 2023;140:413-30. https://doi.org/10.1111/jbg.12768
27. Sobajima T, Yoshimura SI, Maeda T, Miyata H, Miyoshi E, Harada A. The Rab11-binding protein RELCH/KIAA1468 controls intracellular cholesterol distribution. J Cell Biol. 2018;217:1777-96. https://doi.org/10.1083/jcb.201709123
28. Zhang Z, Zhang Z, Oyelami FO, Sun H, Xu Z, Ma P, et al. Identification of genes related to intramuscular fat independent of backfat thickness in Duroc pigs using single-step genome-wide association. Anim Genet. 2021;52:108-13. https://doi.org/10.1111/age.13012
29. Deng L, Jiang C, Chen L, Jin J, Wei J, Zhao L, et al. The ubiquitination of ragA GTPase by RNF152 negatively regulates mTORC1 activation. Mol Cell. 2015;58:804-18. https://doi.org/10.1016/j.molcel.2015.03.033
30. Kadoya M, Sasai N. Negative regulation of mTOR signaling restricts cell proliferation in the floor plate. Front Neurosci. 2019;13:1022. https://doi.org/10.3389/fnins.2019.01022
31. Gangloff YG, Mueller M, Dann SG, Svoboda P, Sticker M, Spetz JF, et al. Disruption of the mouse mTOR gene leads to early postimplantation lethality and prohibits embryonic stem cell development. Mol Cell Biol. 2004;24:9508-16. https://doi.org/10.1128/MCB.24.21.9508-9516.2004

32. Murakami M, Ichisaka T, Maeda M, Oshiro N, Hara K, Edenhofer F, et al. mTOR is essential for growth and proliferation in early mouse embryos and embryonic stem cells. Mol Cell Biol. 2004;24:6710-8. https://doi.org/10.1128/MCB.24.15.6710-6718.2004
33. Laplante M, Sabatini DM. mTOR signaling at a glance. J Cell Sci. 2009;122:3589-94. https://doi.org/10.1242/jcs.051011
34. Kim J, Guan KL. mTOR as a central hub of nutrient signalling and cell growth. Nat Cell Biol. 2019;21:63-71. https://doi.org/10.1038/s41556-018-0205-1
35. Zhang Z, Chen Z, Diao S, Ye S, Wang J, Gao N, et al. Identifying the complex genetic architecture of growth and fatness traits in a Duroc pig population. J Integr Agric. 2021;20:1607-14. https://doi.org/10.1016/S2095-3119(20)63264-6
36. Kools P, Van Imschoot G, van Roy F. Characterization of three novel human cadherin genes (CDH7, CDH19, and CDH20) clustered on chromosome 18q22–q23 and with high homology to chicken cadherin-7. Genomics. 2000;68:283-95. https://doi.org/10.1006/geno.2000.6305
37. Lin J, Wang C, Redies C. Restricted expression of classic cadherins in the spinal cord of the chicken embryo. Front Neuroanat. 2014;8:18. https://doi.org/10.3389/fnana.2014.00018
38. Gong H, Xiao S, Li W, Huang T, Huang X, Yan G, et al. Unravelling the genetic loci for growth and carcass traits in Chinese Bamaxiang pigs based on a 1.4 million SNP array. J Anim Breed Genet. 2019;136:3-14. https://doi.org/10.1111/jbg.12365
39. Wei C, Zeng H, Zhong Z, Cai X, Teng J, Liu Y, et al. Integration of non-additive genome-wide association study with a multi-tissue transcriptome analysis of growth and carcass traits in Duroc pigs. Animal. 2023;17:100817. https://doi.org/10.1016/j.animal.2023.100817
40. Che L, Yang Z, Xu M, Xu S, Che L, Lin Y, et al. Maternal nutrition modulates fetal development by inducing placental efficiency changes in gilts. BMC Genom. 2017;18:213. https://doi.org/10.1186/s12864-017-3601-1
41. Xu Z, Jin X, Cai W, Zhou M, Shao P, Yang Z, et al. Proteomics analysis reveals abnormal electron transport and excessive oxidative stress cause mitochondrial dysfunction in placental tissues of early-onset preeclampsia. Proteomics Clin Appl. 2018;12:1700165. https://doi.org/10.1002/prca.201700165
42. Kunzelmann K, Tian Y, Martins JR, Faria D, Kongsuphol P, Ousingsawat J, et al. Airway epithelial cells—functional links between CFTR and anoctamin dependent Cl– secretion. Int J Biochem Cell Biol. 2012;44:1897-900. https://doi.org/10.1016/j.biocel.2012.06.011
43. Feng M, Wang Z, Liu Z, Liu D, Zheng K, Lu P, et al. The RyR–ClCa–VDCC axis contributes to spontaneous tone in urethral smooth muscle. J Cell Physiol. 2019;234:23256-67. https://doi.org/10.1002/jcp.28892
44. Chen D, Meng W, Shu L, Liu S, Gu Y, Wang X, et al. ANO1 in urethral SMCs contributes to sex differences in urethral spontaneous tone. Am J Physiol Renal Physiol. 2020;319:F394-402. https://doi.org/10.1152/ajprenal.00174.2020
45. Bergamaschi M, Maltecca C, Fix J, Schwab C, Tiezzi F. Genome-wide association study for carcass quality traits and growth in purebred and crossbred pigs. J Anim Sci. 2020;98:skz360. https://doi.org/10.1093/jas/skz360
46. Lee J, Kang JH, Kim JM. Bayes factor-based regulatory gene network analysis of genome-wide association study of economic traits in a purebred swine population. Genes. 2019;10:293. https://doi.org/10.3390/genes10040293
47. Sun WX, Wang HH, Jiang BC, Zhao YY, Xie ZR, Xiong K, et al. Global comparison of gene expression between subcutaneous and intramuscular adipose tissue of mature Erhualian pig. Genet Mol Res. 2013;12:5085-101. https://doi.org/10.4238/2013.October.29.3

https://doi.org/10.5187/jast.2023.e104

48. Montero A, Okada Y, Tomita M, Ito M, Tsurukami H, Nakamura T, et al. Disruption of the fibroblast growth factor-2 gene results in decreased bone mass and bone formation. J Clin Invest. 2000;105:1085-93. https://doi.org/10.1172/JCI8641
49. Wang Z, Guo J, Guo Y, Yang Y, Teng T, Yu Q, et al. Genome-wide detection of CNVs and association with body weight in sheep based on 600K SNP arrays. Front Genet. 2020;11:558. https://doi.org/10.3389/fgene.2020.00558
50. Wong W, Scott JD. AKAP signalling complexes: focal points in space and time. Nat Rev Mol Cell Biol. 2004;5:959-70. https://doi.org/10.1038/nrm1527
51. Casiró S, Velez-Irizarry D, Ernst CW, Raney NE, Bates RO, Charles MG, et al. Genome-wide association study in an F2 Duroc x Pietrain resource population for economically important meat quality and carcass traits. J Anim Sci. 2017;95:545-58. https://doi.org/10.2527/jas.2016.1003
52. Zofkie W, Southard SM, Braun T, Lepper C. Fibroblast growth factor 6 regulates sizing of the muscle stem cell pool. Stem Cell Reports. 2021;16:2913-27. https://doi.org/10.1016/j.stemcr.2021.10.006
53. Armand AS, Laziz I, Chanoine C. FGF6 in myogenesis. Biochim Biophys Acta. 2006;1763:773-8. https://doi.org/10.1016/j.bbamcr.2006.06.005
54. Doukas J, Blease K, Craig D, Ma C, Chandler LA, Sosnowski BA, et al. Delivery of FGF genes to wound repair cells enhances arteriogenesis and myogenesis in skeletal muscle. Mol Ther. 2002;5:517-27. https://doi.org/10.1006/mthe.2002.0579
55. Srikanchai T, Murani E, Phatsara C, Schwerin M, Schellander K, Ponsuksili S, et al. Association of ZYX polymorphisms with carcass and meat quality traits in commercial pigs. Meat Sci. 2010;84:159-64. https://doi.org/10.1016/j.meatsci.2009.08.042
56. Macalma T, Otte J, Hensler ME, Bockholt SM, Louis HA, Kalff-Suske M, et al. Molecular characterization of human zyxin. J Biol Chem. 1996;271:31470-8. https://doi.org/10.1074/jbc.271.49.31470
57. Nix DA, Fradelizi J, Bockholt S, Menichi B, Louvard D, Friederich E, et al. Targeting of zyxin to sites of actin membrane interaction and to the nucleus. J Biol Chem. 2001;276:34759-67. https://doi.org/10.1074/jbc.M102820200
58. Yoshigi M, Hoffman LM, Jensen CC, Yost HJ, Beckerle MC. Mechanical force mobilizes zyxin from focal adhesions to actin filaments and regulates cytoskeletal reinforcement. J Cell Biol. 2005;171:209-15. https://doi.org/10.1083/jcb.200505018
59. Hansen MDH, Beckerle MC. Opposing roles of zyxin/LPP ACTA repeats and the LIM domain region in cell-cell adhesion. J Biol Chem. 2006;281:16178-88. https://doi.org/10.1074/jbc.M512771200
60. Hoffman LM, Nix DA, Benson B, Boot-Hanford R, Gustafsson E, Jamora C, et al. Targeted disruption of the murine zyxin gene. Mol Cell Biol. 2003;23:70-9. https://doi.org/10.1128/MCB.23.1.70-79.2003
61. Sánchez-Roncancio C, García B, Gallardo-Hidalgo J, Yáñez JM. GWAS on imputed whole-genome sequence variants reveal genes associated with resistance to Piscirickettsia salmonis in rainbow trout (Oncorhynchus mykiss). Genes. 2023;14:114. https://doi.org/10.3390/genes14010114
62. Dean JM, He A, Tan M, Wang J, Lu D, Razani B, et al. MED19 regulates adipogenesis and maintenance of white adipose tissue mass by mediating PPARγ-dependent gene expression. Cell Rep. 2020;33:108228. https://doi.org/10.1016/j.celrep.2020.108228
63. Hwang JH, An SM, Kwon SG, Park DH, Kim TW, Kang DG, et al. Associations of the polymorphisms in DHRS4, SERPING1, and APOR genes with postmortem pH in Berkshire

pigs. Anim Biotechnol. 2017;28:288-93. https://doi.org/10.1080/10495398.2017.1279171
64. Zhao YY, Lin YQ, Xu YO. Functional identification of allograft inflammatory factor 1-like gene in luning chicken. Anim Biotechnol. 2018;29:234-40. https://doi.org/10.1080/10495398.2017.1369096
65. Rakita A, Nikolić N, Mildner M, Matiasek J, Elbe-Bürger A. Re-epithelialization and immune cell behaviour in an ex vivo human skin model. Sci Rep. 2020;10:1. https://doi.org/10.1038/s41598-019-56847-4
66. Neustaeter A, Grossi DA, Jafarikia M, Sargolzaei M, Schenkel F. Genome-wide association study for loin marbling score in Canadian Duroc pigs. In: Proceedings of the 10th World Congress of Genetics Applied to Livestock Production; 2014; Vancouver, BC.
67. Kokta TA, Dodson MV, Gertler A, Hill RA. Intercellular signaling between adipose tissue and muscle tissue. Domest Anim Endocrinol. 2004;27:303-31. https://doi.org/10.1016/j.domaniend.2004.05.004
68. Yang W, Liu Z, Zhao Q, Du H, Yu J, Wang H, et al. Population genetic structure and selection signature analysis of Beijing black pig. Front Genet. 2022;13:860669. https://doi.org/10.3389/fgene.2022.860669
69. Falker-Gieske C, Blaj I, Preuß S, Bennewitz J, Thaller G, Tetens J. GWAS for meat and carcass traits using imputed sequence level genotypes in pooled F2-designs in pigs. G3. 2019;9:2823-34. https://doi.org/10.1534/g3.119.400452
70. Naslavsky N, Rahajeng J, Rapaport D, Horowitz M, Caplan S. EHD1 regulates cholesterol homeostasis and lipid droplet storage. Biochem Biophys Res Commun. 2007;357:792-9. https://doi.org/10.1016/j.bbrc.2007.04.022

https://doi.org/10.5187/jast.2023.e104